NONLINEAR CONTACT ANALYSIS TO EVALUATE STRESS ON COMPONENTS OF DENTAL PROSTHESES USING FINITE ELEMENT MODEL

Edson A. Capello Sousa, capello@feb.unesp.br
Elton Carlos Silveira, eltoncsi.silveira@hotmail.com
Bruno Agostinho Hernandez, bhernandez@uol.com.br
Department of Mechanical Engineering - Faculty of Engineering - State University of São Paulo (Unesp)
Av. Luiz Edmundo Carrijo Coube s/n, Bauru, São Paulo, Brazil

Abstract. *The aim of this study was to analyze stress distribution on components of a fixed implant-supported prosthesis, using a Finite Element Model with contact elements. The study analyzed the stress and possible failure of the prostheses components due the contact between the parts. The dental prosthesis is frequently subjected to forces due to the chewing, producing stresses on its structure that are transmitted to the bone. But, the prostheses have internal stress due to the process of fixing the implants to the bone tissue and fastening of prosthesis components. The high values (stresses) can damage and break them. Also, the passive fit between prostheses and their components is considered essential for implant prosthodontic success. Finite Element Analysis has been shown to be very effective in simulating non-linear contact problem, especially in biomechanics problems, and it has been widely used in dental prosthesis analysis with the intention to improve this system. For this analysis, a Finite Element model was constructed including contact mechanics elements. The model simulated a typical mandibular partial fixed framework with two implants. In a mathematic model a framework was screwed on two independent abutments over the implants. The load was applied on three different points of the bar, corresponding to 10 mm, 15 mm and 20 mm from the center to the last implant, towards the free length of the bar. Three alloy materials were studied for the framework: Cobalt-Chromium, Palladium-Silver and Gold. The stresses were observed on the top and bottom sides of the cantilever beam, near the terminal abutment. The stress on the abutments and screws were also observed. The contact elements were applied at the interface of the infrastructure with the abutments and with the screws. It showed the necessity of the contact elements in the analysis of structural projects of prostheses. With the use of contact elements in the simulation model could be observed the influence of the assembling preload of prosthesis. Therefore, it could be seen that the structural behavior of the prosthesis has changed due to loss of screw tightening. It was found that the stress in the prosthetic components changed as a function of assembling preload. The stress distribution has changed in the infrastructure, abutment and screw. The position of the point load application on the cantilever and the type of material of framework were shown to influence the stress distribution in the components. The results clearly showed the importance of the contact elements in the structural analysis of prostheses. Whenever possible, the results of the finite element models were compared with experimental data using strain gauge measurements. This type of analysis has the potential to improve the project of the prosthesis and to reduce the incidence of breakage and injury to the patients.*

Keywords*: Biomechanics, Contact Mechanic problem, Dental prostheses, Strain gauges measurements, Finite Elements Method.*

1. INTRODUCTION

In the biomedical field, there are many adequate clinical solutions for medical problems. However, there are areas, such as bioengineering, in which research has recently achieved much progress. Techniques often used in engineering, which use both experimental and computational simulations, can also be applied to various biomedical applications, such as medicine and dentistry. Techniques commonly used in solving engineering problems prevailed for many years as only experimental analysis. However, with the advent of computers made way for other forms of analysis. Aided by immense progress in mathematical research and development of computer systems, numerical solutions have become formidable force in solving engineering problems. Thus, both experimental and numerical solutions have been effectively used for some time to solve engineering problems, and more recently have been applied to bioengineering.

The methods most commonly used in engineering are: finite element modeling for numerical solutions, and measurement using strain gauges for experimental solutions. Actually, there is no significant advantage between obtaining results through numerical modeling or through experimental analysis. It should be noted that neither technique should replace the other; moreover, it is common to use them in conjunction. In fact, there is consensus among researchers and practitioners that these methodologies are complementary, making them a powerful tool for developing research and technological advances. The relevance of these technologies in bioengineering is accentuated when it comes to applications to medical prostheses. The prosthesis itself is considered to be external to the body and intended to replace a natural function, which has been impaired in the human body. There are several situations in which the prosthesis can be applied. Among these applications are prostheses that provide structural functionality, where mechanical components or assemblies of mechanical components are placed in patients to provide structural

rigidity and receive and absorb mechanical stress. A dental prosthesis is also characterized as a structural prosthesis, making it possible to restore the patients the ability to chew, which result in the application of forces to the prosthesis that are sufficient to cause fractures in the mechanical components of the assembly. Therefore, it should be possible to evaluate the mechanical loads on the components and develop improvement to the structural design of the prosthesis that enhances efficiency and durability.

Skalak (1983), one of the pioneering studies of the use of biomechanics in dental implants, assesses the stresses between the osseointegrated implant and bone tissue. Initially, some researchers; including Rangert et al (1989), Patterson et al (1992), Jaarda et al (1993), Weinberg (1993) and Monteith (1993); used clinical or direct techniques to obtain loads on implants. Experimental techniques greatly simplified the determination of these loads. Photoelasticity was a popular experimental technique used in dentistry, and has been used in research by Milligton Laung (1992), and Waskewicks et al (1994) and White et al (1994). More recently, strain gauges have been used in the structural evaluation of dental prostheses, as cited in Isa and Hobkirk (1995), Carr et al (1996), Isa and Hobkirk (1996) and Hobkirk and Havthoulas (1998). Research by Chao et al (1988), Clelland et al (1993) and Assif et al (1996) has combined the two methods, photoelasticity and strain gauges, to estimate the loading on the prosthesis. Other studies of implant-supported (Branemark implants) fixed prosthesis performed by Hollweg (2000) and Hollweg et al (2001) used strain gauges to assess the loading on the implant/prosthesis assembly. A similar experiment, performed by Jacques (2000) and Jacques et al (2001), assessed the misalignment between the infrastructure and the implants. There are also studies that have used finite element method to evaluate dental prostheses as cited in research by Williams et al (1990), Chen et al (1994), Sertgöz and Güven (1996) and Sertgöz (1997). All of the research to date has focused on evaluating the design of the prosthesis, and in some cases includes modeling of the mandible.

The aim of this study is to evaluate stresses subjected to the mechanical components of dental prostheses. In this study, an implant-supported prosthesis is used for the evaluation of stresses that occur in the infrastructure supported by implants. Evaluations of the prosthesis/implant assembly are performed using a finite element model as well as through experimental analysis using strain gauges. The accuracy of the results obtained by the two methods is also validated.

2. FINITE ELEMENT MODELING WITH MECHANICAL CONTACT

2.1. Geometric Finite Element Model

For this study, it was considered prudent to validate the numerical model, including the mechanical contacts, by comparing previous results obtained from a finite element model of the prosthetic assembly without mechanical contacts, and the results of the experimental prototype using strain gauges. The numerical simulation model for the prosthesis consisted of the infrastructure (bar) supported by abutments (implants) and mounting screws. Three alloys, which were also the subjects of the evaluation in the previous chapter, were analyzed in this study, i.e., Chromium-Cobalt alloy (CoCr), Palladium-Silver alloy (PdAg) and a Gold alloy (Au).

Figures 1 to 3 show the geometric model of the prosthetic assembly used in the numerical simulation. The Finite Element model was developed using ANSYS v10.0 software. It should be noted that the geometry of the prosthesis depends on the physical characteristics of each patient, which determines the placement of implants. The partial denture model is similar to the previously evaluated model, except that it includes additional elements representing the contact geometry. Supports are made from the contact with the implants and the bar has a free (cantilevered) end where the loading is applied. The FEM model must preserve the mechanical characteristics of the actual prosthetic assembly; therefore, the material properties and geometry should be maintained in the model. As already noted, the weight and geometry of the prosthesis were measured, ensuring consistency between the Finite Element models and experimental models used previously.

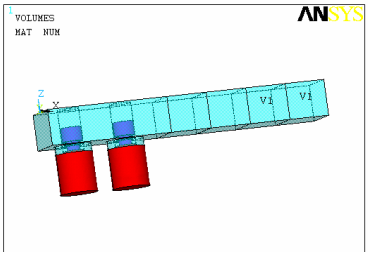

Figure 1 - Geometric Model of Partial Prosthesis - Mechanical Contact

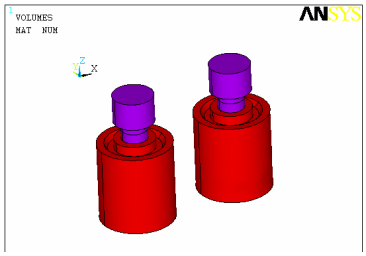

Figure 2 - Prosthesis - Screws and Implants

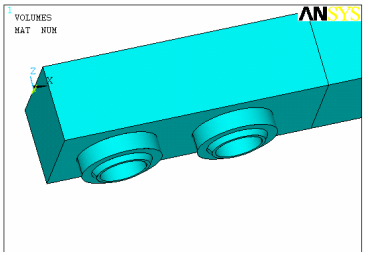

Figure 3 - Details of Constructive Prosthesis - Infrastructure

2.2. Contact Elements

Figure 4 shows the finite element model of the prosthesis and the mesh used in the analysis. The model uses cubic and tetrahedral elements using high-order interpolations. Solid95 and Solid92 elements are used in the Ansys program,

as defined in the previous section. In general, the mesh definition corresponds to the model in the previous chapter, where the model had region of mapped mesh and a region of free mesh. The free end of the infrastructure is modeled with a mapped mesh, while the intersection between the infrastructure and the implants uses a free mesh. The free mesh near the implants facilitates the definition of the local non-uniform geometry. This adjustment of the mesh is important because it optimizes of the number of elements in the final mesh, allowing a reduction in computational costs and calculation time.

Element types Conta174 and Targe170 used for the contact regions. Conta174 is a 3D contact element used to connect deformable surfaces in three-dimensional models. This contact element is defined together with the Targe170 element, whose contact must be defined on the surface that forms the contact pair. It should be noted that in the details of the mesh, shown in Figure 5, the generated meshes are coincident. This occurs because the surfaces and mesh are defined and generated separately to make the contact between the parts.

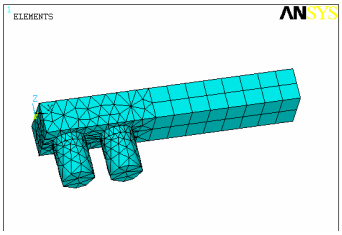

Figure 4 - Mesh of the Finite Element Model

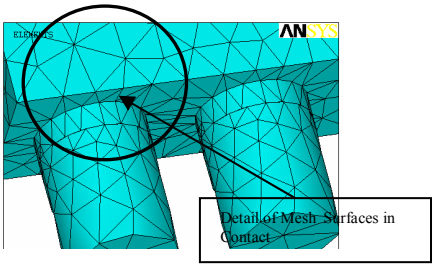

Figure 5 - Finite Element Model - Mesh on Distinct Surfaces

The following figures show the definition of contact elements in Finite Element model. The contact elements are usually defined as contact pairs, having two surfaces that interact to maintain mechanical contact between the structural components. Thus, one should define two regions of contact for each contact pair. Figures 6, 7 show the definition of the contact element for the abutments. In this case, the Targe170 element is used. Figure 6 shows the elements defined for the contact region, while Figure 7 shows the surface of the contact elements. Figure 8 shows the region in which the contact elements must interact with the other contact part. Therefore, as shown, one side of the contact elements is defined for the abutments and must interact with its counterpart located in the infrastructure. Figures 9 and 10 show the region where the elements will be defined for the infrastructure.

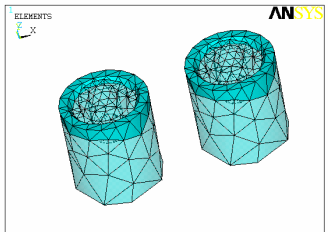

Figure 6 - Contact Region - Intermediates

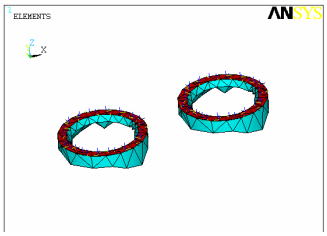

Figure 7 - Contact Region - Intermediates - Targe170 Element

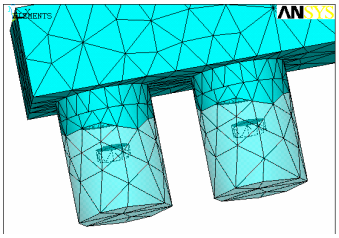

Figure 8 - Contact Region - Prosthesis - Intermediate (Abutment)

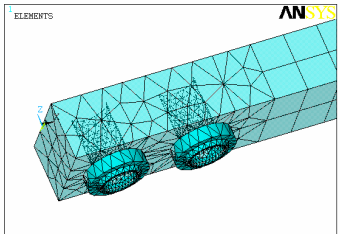

Figure 9 - Contact Region - Prosthesis

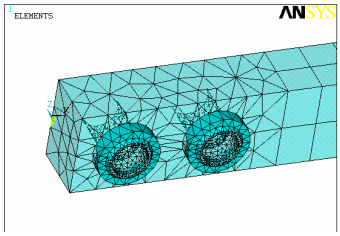

Figure 10 - Contact Region - Prosthesis - bottom detail

Figure 11 shows the layout of the contact elements. This side of the contact pair is defined by the Conta174 element. It should be noted that the contact pairs, Targe170 and Conta174 work together to define each side of the contact surface. Figure 12 shows the final configuration of contact elements laid out for the mechanical contact between the abutments and the infrastructure of the prosthesis. Next, the region in which the screws make contact with other parts of the structure must be defined. Figures 13 and 14 show the region where the screw head should make contact with the infrastructure of the prosthesis. It should be noted that there is a small ring where the screw head is supported and receives loading from infrastructure. This area is defined to maintain a bonded contact between the screw and the infrastructure, and only through this area can forces be transferred between these components. It should also be noted

that there is a gap between both the head and shaft of the screw and the infrastructure, as identified in Figure 6.14. Therefore, these regions do not maintain contact with each other, as in the case of the actual structure. Figure 6.15 shows detail of the region where the screw engages with the infrastructure.

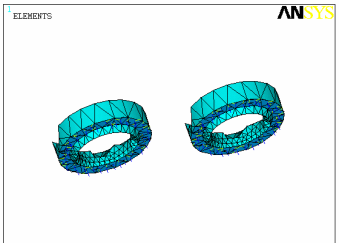

Figure 11 - Contact Region - Prosthesis - Conta174 Element

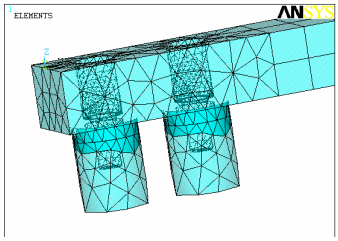

Figure 12 - Contact Region - Prosthesis and Intermediary (Abutment) - Contact Region

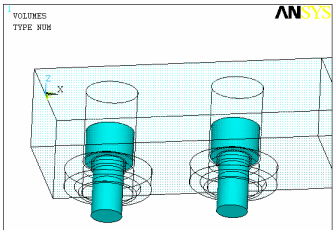

Figure 13 - Gap regions - Screw - Prosthesis

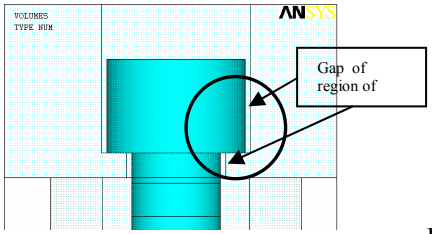

Figure 14 - Gap regions - Screw - Prosthesis - Detail

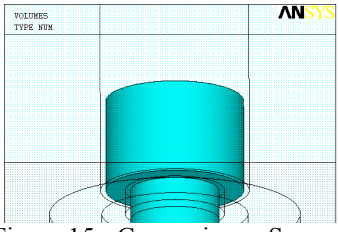

Figure 15 - Gap regions - Screw - Prosthesis

Figures 16 and 17 show the areas where the contact must occur between the screw and infrastructure. Figure 16 shows the area where the head of the screw makes contact with the infrastructure, while Figure 17 shows where this area is supported by the infrastructure. Finally, Figures 18, 19 and 20 show the regions where the screw must interact with the abutments. Figure 18 shows the clearance between the shaft of the screw and the abutments. The Figures 19 and 20 show the areas where the shaft of the screw must maintain frictional/bonded contact with the abutment. This region would be represented by the screw thread incorporated into the abutment.

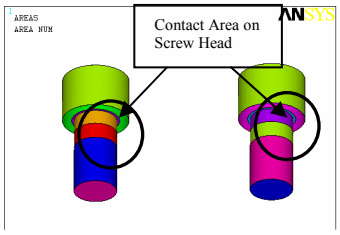

Figure 16 - Contact Region – Contact Area - Screw - Prosthesis

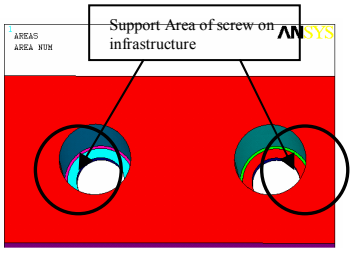

Figure 17 - Contact Region - Contact Area - Screw - Prosthesis – Prosthesis Detail

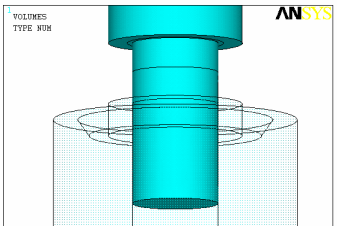

Figure 18 - Region - Screw - Intermediaries

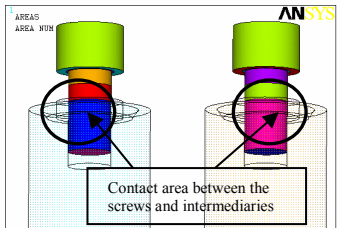

Figure 19 - Region of Contact - Contact Area - Screw - Intermediaries

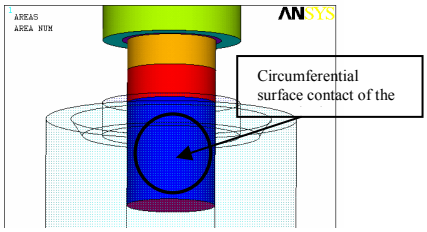

Figure 20 - Region of Contact - Contact Area - Bolt - Details Intermediate

2.3. Boundary Conditions

It is necessary to identify and apply all the mechanical loading and boundary conditions (connections and supports) to model, so as to replicate the conditions to which the actual structure is subjected. From a clinical perspective, it is considered that the implants completely bond to the bone through the process of osseointegration. Therefore, it is considered that the implants are fully integrated with the bone along its lower surface, i.e. no deformation occurs along this surface. This assumption is also consistent with the configuration of the experimental prototype. The chewing forces are characterized by an external force applied at predefined points of 10, 15 and 20 mm along free (cantilevered)

end of infrastructure measured from the last implant. Figure 21 shows the Finite Element model and its boundary conditions, such as the connections to the bone and external loading.

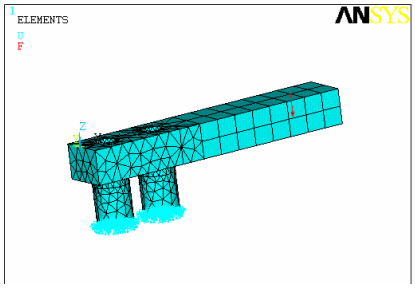

Figure 21 - Boundary Conditions of the Finite Element Model

3. NUMERICAL RESULTS OF FINITE ELEMENT NUMERICAL MODELS - MODEL WITH AND WITHOUT MECHANICAL CONTACTS

In the previous chapter a detailed validation of the numerical Finite Element model was performed comparing computational results with experimental data. As previous stated, this Finite Element model has been improved with the addition of elements that describe the mechanical contact between components of the prosthesis. Therefore, the purpose of this section is to validate the results from the numerical simulation using a Finite Element model of the prosthesis without mechanical contacts and a similar model with mechanical contacts. The numerical results of FEM model with contacts should be compared to data obtained through the simplified FEM model without contacts to verify the quality of results obtained in the model with contacts. Whenever possible the analytical results to be used in the analysi should be estimated.

In previous analyzes the deformations in the free (cantilevered) region of the bar were compared with results obtained from the strain gauges placed on the upper and lower regions of the bar next to the last implant support. The analysis and results presented in this section must follow the same sequence, for in addition to defining the region of larger requirement through out the free region of the bar, this region has a more uniform stress distribution, as shown in Figure 22. It should be noted that the mechanical contact between the components of the prosthesis, i.e. the bar, abutments and screws, should not significantly alter the stress distribution on the bar. As previously observed, the stress distribution in the bar varies with depth, from tensile stress (positive stress) at the top of the bar to compressive stress (negative stress) at the bottom of the bar, as shown in Figure 22. These stresses are also associated with tensile and compressive deformations depending on the region being observed

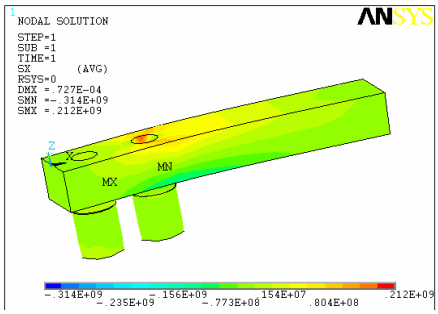

Figure 22 - Distribution of Stresses on the Implant - Mechanical Contacts

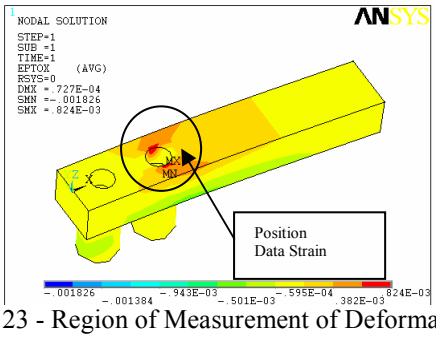

Figure 23 - Region of Measurement of Deformations - Mechanical Contact

For this first analysis to validate the numerical results, the top region of the bar should be observed, by the deformation values obtained in both the Finite Element Model with mechanical contact as in the simplified model without mechanical contact, Figure 23 shows the strains produced by bending the prosthesis, and identifies an area where the strains from the numerical analysis exhibit similar values to those found in the experimental evaluations. However, it should be noted that in the case of the experimental evaluations, this region was precisely defined a points where strain gauges were installed to obtain the experimental data and these same point locations were used to obtain numerical data. In many cases, the position of strain gauges did not coincide with the position of the FEM nodal point, and therefore required the interpolation of data from adjacent nodes to estimate the deformation at the equivalent location of the stain gauge. In the analysis in this section, a single geometric point was defined where strains were measured or evaluated for all three types of materials. This standardized point was located 5 mm from the center of the last implant, in the direction of the free (cantilevered) end of the bar. The location of this point was selected using the following criteria; 1) avoid the region of concentrated tensile stresses, 2) avoid the region where the prosthesis is attached to the implants, and 3) align with a FEM nodal point to facilitate direct reading without interpolation. The experimental results were also calculated at the same point. It is important to note that the evaluations were done with

three alloys, CoCr, PdAg and Au, using the same geometry in all cases; h = 4.4 mm and b = 6.4 mm, which refer to the respective depth and breadth of the bar (infrastructure).

Table 1 - Results of Deformation - Numeric Data - FEM Model

Distance from the point of load application L_f (mm)	Cobalt-Chromium Bar (CoCr)			Palladium-Silver Bar (PdAg)			Gold Bar (Au)		
	Tensile Strain ε (μ)			Tensile Strain ε (μ)			Tensile Strain ε (μ)		
	Analytic data	Numerical Data with no Contact	Numerical Data with Contact	Analytic data	Numerical Data with no Contact	Numerical Data with Contact	Analytic data	Numerical Data with no Contact	Numerical Data with Contact
10	111,07	106,56	103,59	186,25	178,60	173,51	220,11	211,09	204,98
15	222,13	210,52	206,16	372,50	352,96	345,38	440,22	417,18	408,04
20	333,20	315,70	310,09	558,74	529,38	519,52	660,33	625,71	613,79

The results from both versions of the FEM numerical models present better correlation when compared to the analytical results. This can be explained by the fact that the analytical results are simplified and do not take into account the effect of the stress concentration cause by the mounting of the prosthesis. In every case investigate, the strains obtained for the model with mechanical contacts were shown to be smaller than those strains obtained for the simplified models without mechanical contacts.

4. COMPARISONS OF THE RESULTS OF STRAIN FOR FINITE ELEMENT MODELS WITH AND WITHOUT MECHANICAL CONTACTS

4.1. Deformation Results in Infrastructure

Verification of numerical models can be achieved by observing the distribution of strain in infrastructure. As already noted, the structural behavior of the bar, or the infrastructure, of the prosthesis is not significantly influenced by the contact between components. Therefore, it can be expected that the distribution of stresses and strains will be quite uniform and behave similarly along the bar.

Figures 24, 25 and 26 show the strains analyzed for each of the alloys CoCr, PdAg and Au, respectively. In this first group of results, the strains are shown for the simplified model without mechanical contacts. The results are obtained for various loading configurations, which are generated by varying the position of the applied load along the bar. It should also be noted that the strains are longitudinal, i.e., strains in the x direction (εx) along the bar. The other group of results, shown in Figures 27, 28 and 29, represents the strains obtained from the FEM model with mechanical contacts for the alloys of CoCr, PdAg and Au, respectively. Once again, the results are observed for various loading configurations, which are generated by varying the position of the applied load along the bar.

By observing the results from the two models for the CoCr alloy, as shown in Figures 24 and 27, it can clearly be seen that the result for the strains are very similar. The distribution of the strains is very similar for both models, and there is also good coincidence in the regions of maximum strain. There is also strong correlation between the maximum strains produced in each of the two models for each variation in the applied load. For the model without mechanical contacts, the strain for varying the position of the load (Lf= 10 mm, 15 mm and 20 mm), are respectively 364με, 565με and 767με, while for the case of the model with mechanical contacts the corresponding strains are 389με, 604με and 824με. In each of these cases the difference between the results is the order of 6%, and therefore it can be considered that adding the contacts to the model does not significantly affect the results for stain. This behavior is observed for the PdAg alloy (Figures 25 and 28) and the Au alloy (Figures 26 and 29).

- Strain on the Contact prosthesis on FEM Model

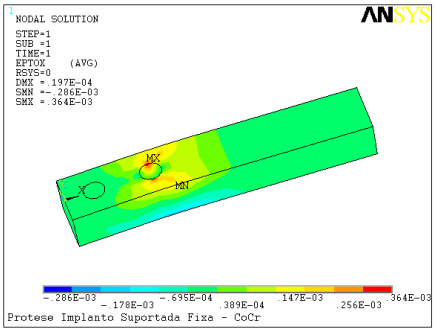

Figure 24a - Position of Load - Lf = 10 mm

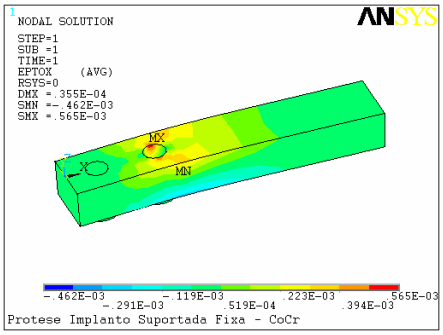

Figure 24b – Position of Load - Lf = 15 mm

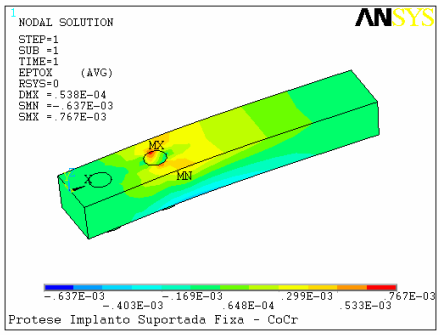

Figure 24c – Position of Load - Lf = 20 mm

Figure 24 - Nodal Strain - CoCr Alloy Prosthesis - Without Mechanical Contacts

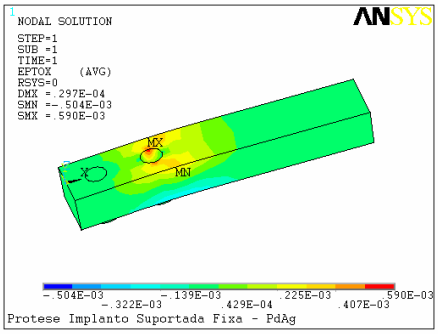

Figure 25a - Position of Load - Lf = 10 mm

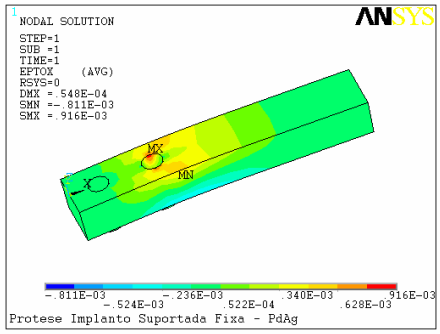

Figure 25b - Position of Load - Lf = 15 mm

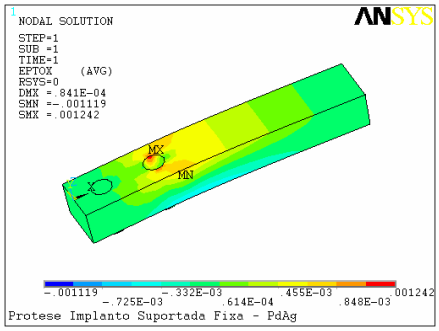

Figure 25c - Position of Load - Lf = 20 mm

Figure 25 - Nodal Strains - PdAg Alloy Prosthesis - Without Mechanical Contacts

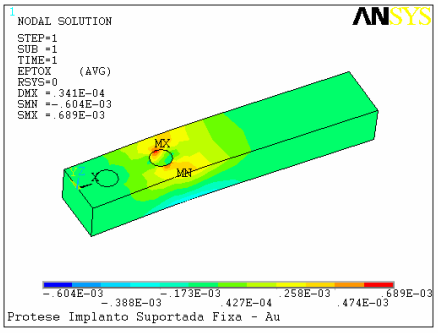

Figure 26a - Position of Load - Lf = 10 mm

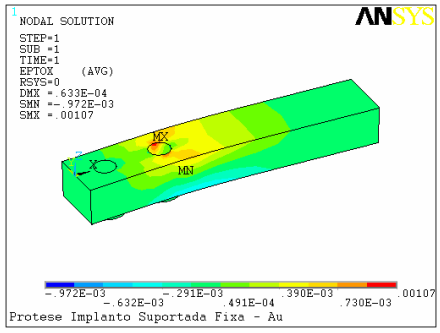

Figure 26b - Position of Load - Lf = 15 mm

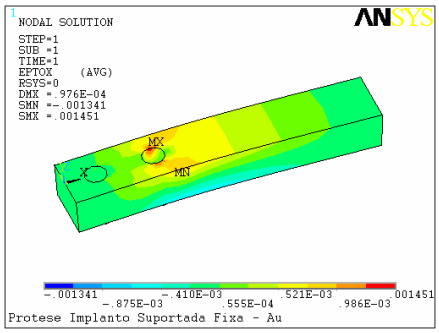

Figure 26c - Position of Load - Lf = 20 mm

Figure 26 - Nodal Strains - Au Alloy Prosthesis - Without Mechanical Contacts

- Strains on the Prosthesis for FEM Model with Mechanical Contacts

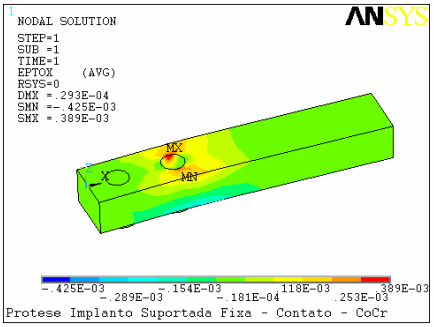

Figure 27a - Position of Load - Lf = 10 mm

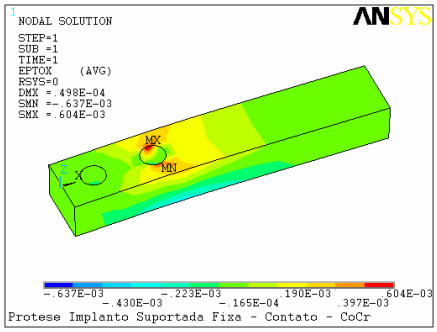

Figure 27b - Position of Load - Lf = 15 mm

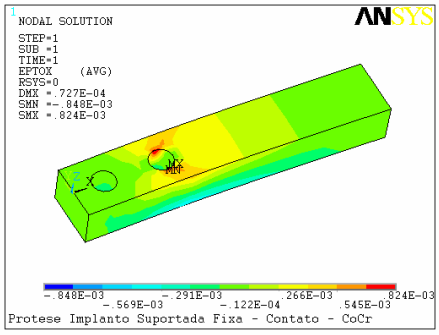

Figure 27c - Position of Load - Lf = 20 mm

Figure 27 - Nodal Strains - PdAg Alloy Prosthesis - with Mechanical Contacts

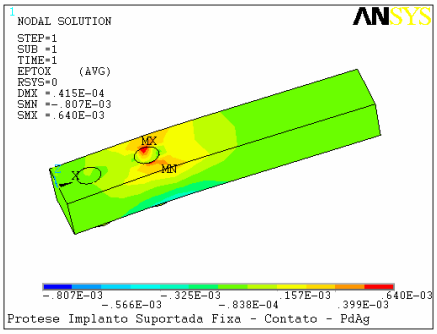

Figure 28a Position of Load - Lf = 10 mm

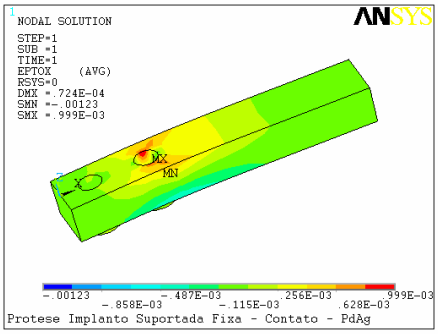

Figure 28b Position of Load - Lf = 15 mm

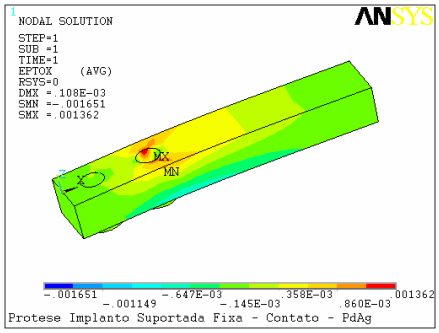

Figure 28c - Position of Load - Lf = 20 mm

Figure 28 - Nodal Strains - PdAg Alloy Prosthesis - with Mechanical Contacts

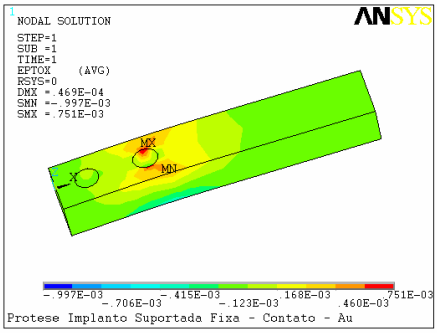

Figure 29a - - Position of Load - Lf = 10 mm

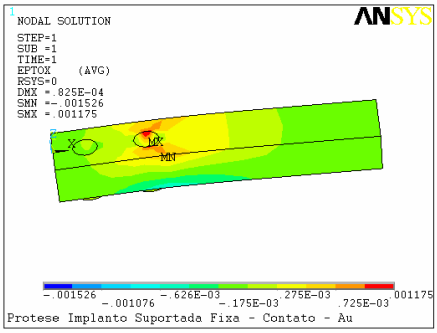

Figure 29b - - Position of Load - Lf = 15 mm

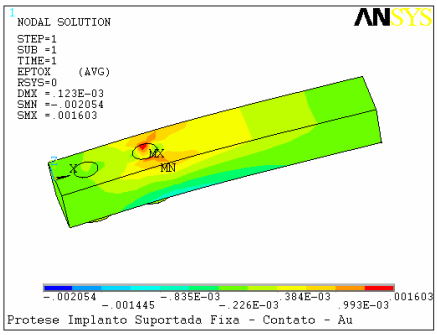

Figure 29c - - Position of Load - Lf = 20 mm

Figure 29 Nodal Strains - Au Alloy Prosthesis - with Mechanical Contacts

In the next section the attention is turned to the abutment (intermediaries) where a comparison is made of the distribution of strains for both boundary conditions, i.e., with and without mechanical contact.

4.2. Results of Analysis about Strains in the Intermediate (Abutments)

In the similar procedure done in previous section, the deformation of the intermediate, obtained by the finite element model without mechanical contact and mechanical contact is evaluated. In these analisys, deformations were observed on both sides of intermediaries, in a position located immediatly below the infrastructure of the prosthesis, see Figure 30. This figure shows the geometric model, where are identified the faces, which the abtuments strains were observed. This position also identifies the point where the numerical results in finite element model with and without contact mechanic, were observed. It should be noted that the distortion of intermediate shown in the following sections were obtained with the Z axis direction (εz). Because the geometry of the prosthesis and loading shown, this is the direction where it should be concentrated higher strain intensity. Furthermore, it is the direction where the stresses and strains are more sensitive to variation of forces. In the following analysis, it should be noted that the faces 0 and 1 are closer to the free end of the bar, while faces 2 and 3 are positioned at the end of the bar opposite the free region where the load is applied. These analysis compare the strain results of the abutments using the Finite Element models with and without contact mechanic. Figures 31 and 32, shows the numerical results for the problem without mechanical contact obtained for each of cobalt chromium alloy (CoCr) and Palladium-Silver (PdAg), respectively. That is, in this modeling, Finite Element models are simplified, where all the bodies are welded to each other. In each set there are three figures

(identified as a) b) c)), where are shown the strains obtained for each loading position at distances of 10mm, 15mm and 20mm, respectivaly, measured from last implant toward to the point of load application.

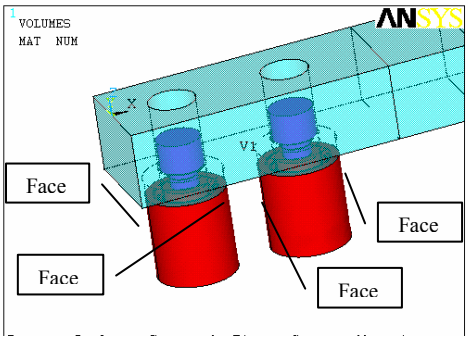

Figure 30 - Faces Observation of Deformation in Intermediates

These results are similar to those presented in the previous cases by analyzing experimental data. But in this case, the geometries of the numerical models are the same for all alloys. Therefore, numerical values can not be effectively compared, but only the behavior of the strain. Figures 31 and 32 shows the strains obtained with the Finite Element model including contact mechanic. In these figures are shown the results for each of alloy CoCr and PdAg, respectively. Unlike what was observed in the results for the infrastructure (bar) of the prosthesis shown in the previous section, the results of deformations for intermediates in the models without contact mechanic (Figures 29 and 30) and contact mechanic (Figures 33 and 34) are actually divergent.

- Numerical Results for Abutments - Without Mechanical Contacts

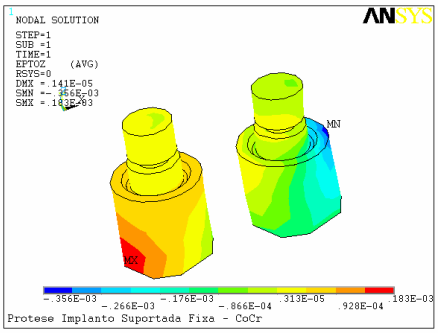

Figure 31a - Position of the Load - Lf = 10 mm

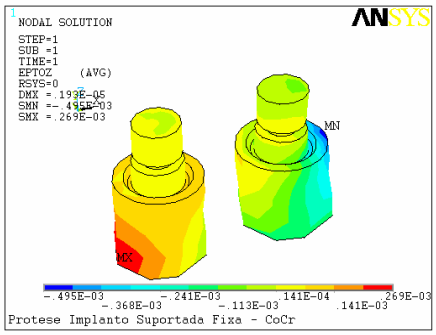

Figure 31b - Position of the Load - Lf = 15 mm

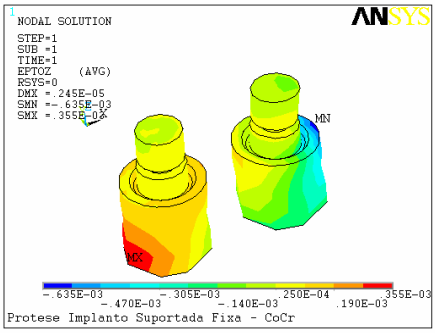

Figure 31c - Position of the Load - Lf = 20 mm

Figure 31 – Strains on Abutments – CoCr Alloy Prosthesis - Without Mechanical Contacts

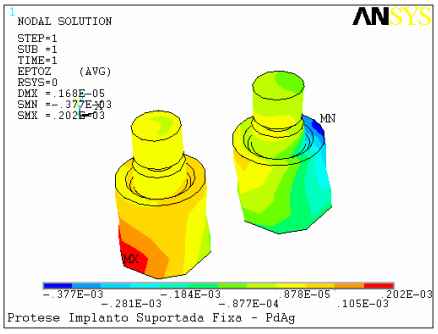

Figure 32a - Position of the Load - Lf = 10 mm

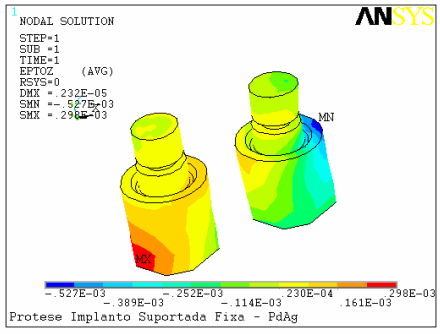

Figure 32b - Position of the Load - Lf = 15 mm

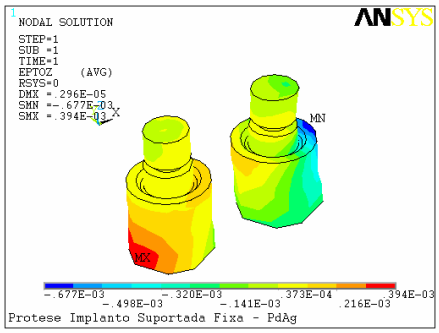

Figure 32c - Position of the Load - Lf = 20 mm

Figure 32 - Strains on Abutments – PdAg Alloy Prosthesis - Without Mechanical Contacts

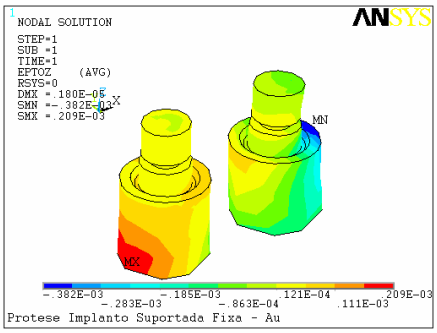

Figure 33a - Position of the Load - Lf = 10 mm

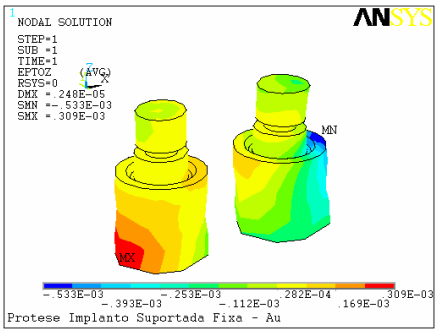

Figure 33b - Position of the Load - Lf = 15 mm

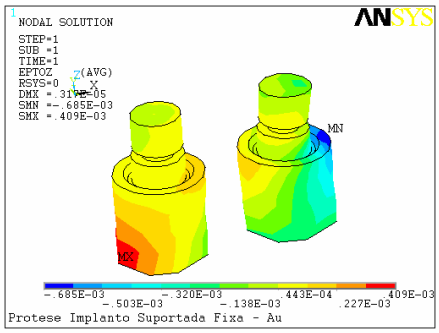

Figure 33c - Position of the Load - Lf = 20 mm

Figure 33 - Strains on Abutments – Au Alloy Prosthesis - Without Mechanical Contacts

- Numerical Results for Abutments - With Mechanical Contacts

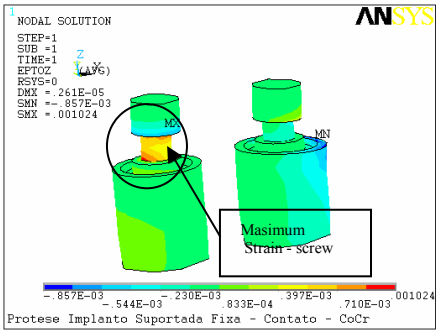

Figure 34a - Position of the Load - Lf = 10 mm

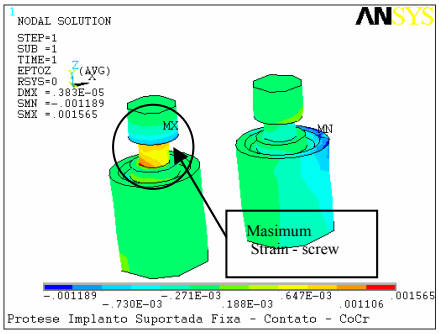

Figure 34b - Position of the Load - Lf = 15 mm

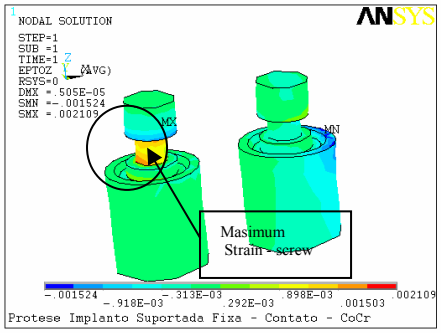

Figure 34c - Position of the Load - Lf = 20 mm

Figure 34 - Strains on Abutments – CoCr Alloy Prosthesis - With Mechanical Contacts

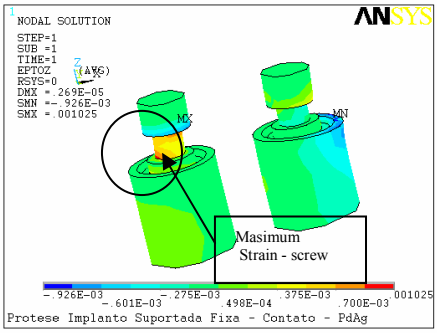

Figure 35a - Position of the Load - Lf = 10 mm

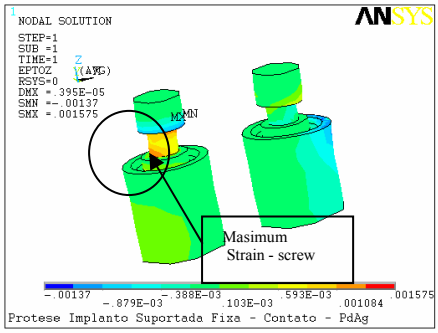

Figure 35b - Position of the Load - Lf = 15 mm

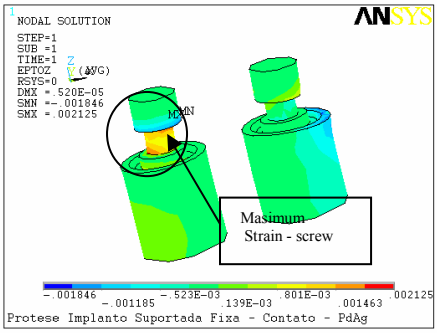

Figure 35c - Position of the Load - Lf = 20 mm

Figure 35 - Strains on Abutments – PdAg Alloy Prosthesis - With Mechanical Contacts

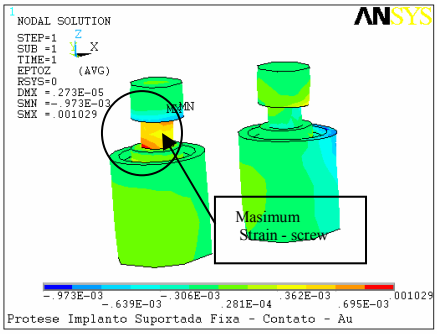

Figure 36a - Position of the Load - Lf = 10 mm

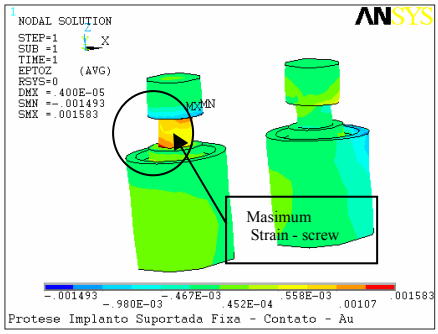

Figure 36b - Position of the Load - Lf = 15 mm

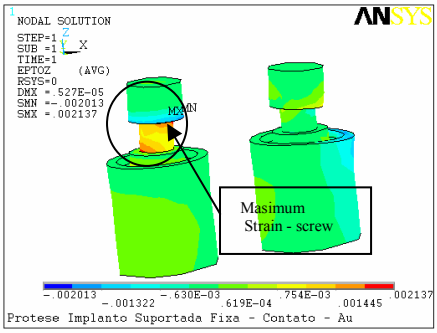

Figure 36c - Position of the Load - Lf = 20 mm

Figure 36 - Strains on Abutments – Au Alloy Prosthesis - With Mechanical Contacts

In this study, a Finite Element model that included mechanical contacts was implemented in the analysis of prostheses. The focus of the study was to observe the results of strains in the prosthetic assembly when the Finite Element model includes mechanical contacts in the analysis, and to determine the influence of these contacts on the structural behavior of the prosthesis. It could be shown that there were significant differences in the resulting strains between the simulation models with, and without, mechanical contacts, as well as the importance of including these contacts in the model to better represent the strains in the actual prosthetic assembly. A natural evolution and improvement of the Finite Element model used to date would be to include the pre-loading from the screws on the assembly in the analysis. A model implementing mechanical contacts would be required to analyze this pre-loading condition. Therefore, further research should be performed to evaluate the implementation of pre-loading in the structural analysis of the prosthesis.

5. REFERENCES

Assif D., Marshak B., Horowitz A., 1996, "Analysis of Load Transfer and Stress Distribution by an Implant Supported Fixed Partial Denture". The Journal of Prosthetic Dentistry, v.75, n.3, p.285-291.

Carr A. B., Brunski J. B., Hurley E., 1996, "Effects of Fabrication, Finishing, and Polishing Procedures on Preload in Prostheses Using Conventional "Gold" and Plastic Cylinders". The International Journal of Oral & Maxillofacial Implants, v.11, n.5, p.589-598.

Chao, Y., 1988, "A Study into the Use Chromium-Cobalt Alloy for Constructing the Framework for Osseointegrated Prostheses". Clinical Materials, v.3, p.309-315.

Chen J., Lu X., Payder N., Akay H. U., Roberts W. E., 1994, "Mechanical Simulation of the Human Mandible with and without an Endosseous Implant". Medical Engineering Physical, v.16, p.53-61.

Clelland N. L., Gilat A., McGlumphy E.A., Brandley W. A., 1993, "A Photoelastic and Strain Gauge Analysis of Angled Abutments for an Implant System". The International Journal of Oral & Maxillofacial Implants, v.8, n.1, p.541-548.

Hobkirk J. A., Havthoulas T. K., 1998, "The Influence of Mandibular Deformation, Implant Numbers, and Loading Position on Detected Forces in Abutments Supported Fixed Implant Superstructure". The Journal of Prosthetic Dentistry, v.80, n.2, p.169-174.

Hollweg H., 2000, "Análise da Passividade de Adaptação de Infra-Estruturas para Prótese Fixa Implanto-Suportada, Através do Uso de Extensômetros". Bauru: Faculdade de Odontologia de Bauru, Universidade de São Paulo, Tese (Doutorado).

Hollweg H., Rubo J. H., Jacques L. B., Capello Sousa E. A., 2001, "Passivity of Fit of Implant Supported Frameworks, Using Strain Gauge Measurements". Journal of Dental Research, AADR Abstracs, v.80, p.101.

Isa Z. M, Hobkirk J. A., 1995, "The Effects of Superstructure Fit and Loading on Individual Implant Units. Part 1: The effects of Tightening the Gold Screw and Placement of a Superstructure with Varying Degrees of Fit". European Journal Prosthodontic Restoring Dentistry, v.3, n.6, p.247-253.

Isa Z. M., Hobkirk J. A., 1996, "The Effects of Superstructure Fit and Loading on Individual Implant Units. Part 2: The effects of Loading a Superstructure with Varying Degrees of Fit". European Journal Prosthodontic Restoring Dentistry, v.4, n.1, p.11-14.

Jacques L. B., 2000, "Análise do Estresse Gerado em Componentes de Prótese Fixa Implanto-Suportada, Através do Uso de Extensômetros". Bauru: Faculdade de Odontologia de Bauru, Universidade de São Paulo, Tese (Mestrado).

Jacques L. B., Rubo J. H., Hollweg H., Capello Sousa E. A., 2001, "Stress Distribuition on Fixed Implant Supported Prostheses, Using Strain Gauge Measurements". Journal of Dental Research, AADR Abstracs, v.80, p.101.

Milligton N. A., Laung T., 1992, "Stress on an Implant Superstructure in Relation to its Accuracy of Fit". Journal Dent. Res., v.71, n.108, p.529-537.

Monteith B. D., 1993, "Minimizing Biomechanical Overload in Implant Prostheses: A Computerized Aid to Design". The Journal of Prosthodont Dentistry, v.5, p.495-502.

Patterson E.A., Johns R.B., 1992, "Theoretic analysis of the Fatigue Life of Fixture Screws in Ossointegrated Dental Implants". The International Journal of Oral & Maxillofacial Implants, v.7, n.1, p.26-34.

Sertgöz A., 1997, "Finite Element Analysis Study of the Effect Superstructure Material on Stress Distribuition in an Implant-Supported Fixed Prothesis". The International Journal of Prosthodontics, v.10, n.1, p.19-27.

Sertgöz A., Güvener S., 1996, "Finite Element Analysis of the Effect of Cantilever and Implant Length on Stress Distribution in an Implant-Supported Fixed Prosthesis". The Journal of Prosthetic Dentistry, v.12, p.165-169.

Skalak, R., 1983, "Biomechanical Considerations in Osseointegrated Prostheses". The Journal of Prosthetic Dentistry, v.49, n.6, p.843-848.

Waskewicks G. A., Ostrowski J. S., Parks V. J., 1994, "Photoelastic Analysis of Stress Distribution Transmitted from a Fixed Prostheses Attached to Osseointegrated Implants", The International Journal of Oral & Maxillofacial Implants, v.9, n.4, p.405-411.

Weinberg L. A., 1993, "The Biomechanic of Force Distribution in Implant Supported Prostheses", The International Journal of Oral & Maxillofacial Implants, v.8, n.1, p.19-31.

White S. N., Caputo A. A., Anderkvist T., 1994, "Effect of Cantilever Length on Stress Transfer by Implant Supported Prostheses", Journal Prosth. Dent., v.71, n.5, p.493-499.

6. RESPONSIBILITY NOTICE

The authors are the only responsible for the printed material included in this paper.